5-2020

Thiol-induced degradation of hydrogels utilizing multiresponsive dithiomaleimides crosslinkers

Kundu Thapa

The University of Southern Mississippi

Thiol-induced degradation of hydrogels utilizing multiresponsive dithiomaleimides crosslinkers

by

Kundu Thapa

A Thesis
Submitted to the Honors College of
The University of Southern Mississippi
in Partial Fulfillment
of the Requirement for the Degree of
Bachelor of Science
in the Department of Polymer Science and Engineering

May 2020

Approved by:

_____

Yoan C. Simon, Ph.D., Thesis Adviser
School of Polymer Science and Engineering

_____

Derek Patton, Ph.D., Director
School of Polymer Science and Engineering

_____

Ellen Weinauer, Ph.D., Dean
Honors College

Abstract

Hydrogels are hydrophilic, three-dimensional materials used as platforms for various biomedical applications such as drug delivery, biosensors, or as scaffolds in tissue engineering. The ability to degrade on demand in response to biological cues is particularly attractive whether dealing with microgels or if one aims to release an active ingredient from a scaffolding material. For instance, many cancer-remediation drug delivery platforms leverage the high concentration of glutathione, a thiol-containing tripeptide, found in cancerous cells. In this work, poly(ethylene glycol) acrylate hydrogels were fabricated using dithiomaleimide (DTM) moieties. DTMs are known to undergo thiol-exchange reactions favoring the dissolution of the hydrogel in the presence of thiols. Herein, we study the role of DTM functionality, and thereby crosslink density, on the mechanical properties of these hydrogels and the rate of dissolution in the presence of thiols including glutathione using rheology and nuclear magnetic resonance (^{1}H NMR). The use of DTM as a crosslinker in multi-responsive hydrogels bears great promise for the creation of stimuli-addressable biomaterials.

Keywords: PEG acrylate hydrogel, dithiomaleimide, glutathione, degradation

Dedication

To my family, especially my sisters, Samaj Thapa, Niku Thapa,and Kundan Thapa for your endless love and support. To my graduate student, Brad Davis, who always supported and encouraged me throughout my undergraduate research journey. I would never have gotten as far as I have without your guidance and motivation. To my advisor, Dr. Yoan Simon for always believing in me and giving me the opportunity to start my undergraduate research journey.

Acknowledgements

I wish to acknowledge the support and advice from my graduate student, Brad Davis; the Wiggins, Patton, and Nazarenko Research Groups; and my fellow undergraduates, Elina Ghimire, Shradha Bhatta, Nabina Lama, and Yumi Maharjan. I would like to thank Rahul Shankar for rheological measurements and valuable discussions. Last but not the least, my advisor Dr. Yoan Simon, Dr. Sarah Morgan, and Dr. Jeffrey Wiggins.

Table of Contents

List of Figures

List of Abbreviations

ACS	American Chemical Society
PEG	Poly(ethylene glycol)
UV	Ultraviolet
DMPA	2,2-dimethoxy-2-phenyl acetophenone
GSH	Glutathione
DTM	Dithiomaleimide
NMR	Nuclear magnetic resonance
THF	Tetrahydrofuran
$MgSO_4$	Magnesium sulfate
EtOAc	Ethylacetate
DCM	Dichloromethane
MeOH	Methanol
TEA	Triethylamine
HCl	Hydrochloric acid
EGDMA	Ethylene glycol methacrylate
PBS	Phosphate buffer saline
DMA	Dynamic mechanical analysis
Pa	Pascal
s	second
K	Kelvin
mL	milliliter

J	Joule
G′	Storage modulus
G″	Loss modulus

Chapter 1: Introduction

Hydrogels are three-dimensional hydrophilic polymeric networks which are known to absorb large volumes of water without dissolving.[1] Hydrogels have gained great interest in the past 50 years in various biomedical applications including controlled therapeutic delivery[2] and as matrices and scaffolds in tissue engineering.[3] The functional groups present in the backbone dictate their hydrophilic nature, contributing to their ability to become hydrated and swollen. Hydrogels networks are either crosslinked physically or chemically via covalent bonds, making them insoluble in aqueous media.[4] Both natural and synthetic polymers can be used to form hydrogels. As compared to natural hydrogels, synthetic hydrogels can be more easily manipulated either with structure or chemistry to control the properties. Most natural hydrogels are based on proteins, such as collagen,[5] gelatin,[6] and polysaccharides,[7] whereas synthetic hydrogels are often made of poly(acrylate),[8] poly(acrylamide),[9] and poly(ethylene glycol).[10] These hydrogels can be tailored and controlled precisely to achieve a broad range of properties such as mechanical flexibility, thermal stability, degradation rate, swelling behavior etc.

Photopolymerization is one of the fastest and most controllable method of preparing hydrogels using visible or ultraviolet (UV) light in the presence of photoinitiators.[11] Photoinitiators are light-sensitive materials which absorb light at specific wavelength to generate free radicals. The free radicals then initiate the polymerization to form fully crosslinked hydrogels. The major photoinitation mechanisms for photolysis are photocleavage, hydrogel abstraction and cationic photopolymerization. Hydroxyalkylphenones, benzoin, benziketals, and acetophenone derivatives initiators undergoes polymerization by cleavage pathways.[12] Poly(ethylene

glycol) acrylate based hydrogels are mainly photopolymerized using acetophenone derivates such as 2,2-dimethoxy-2-phenyl acetophenone[13] and 2-hydroxy-2-methylpropiophenone. These photoinitators generates free radicals either via homolytic cleavage or via hydrogel abstraction as shown in Fig. **1**.

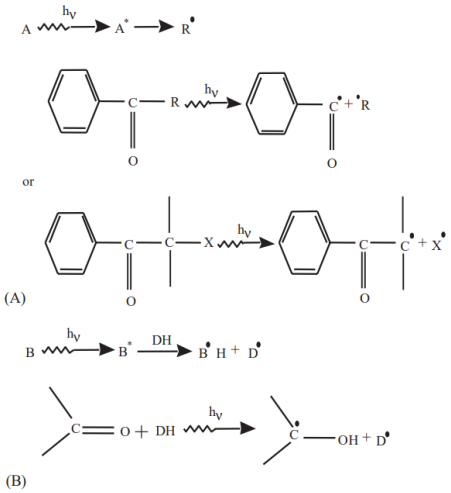

Fig. **1** Photoinitiation mechanism for radical photopolymerization. (A) Photoinitiation by homolytic cleavage. (B) Photoinitiation by hydrogel abstraction.[11]

Hydrogels that can undergo gel-sol phase transition and volume transitions with response to certain external stimuli are called stimuli-responsive hydrogels. Because of their unique ability to respond to environmental cues, there is a growing interest in stimuli-responsive polymer hydrogels in therapeutic drug delivery platforms.[14-15] These types of hydrogels show various changes with external stimuli such as pH,[16,17,18] redox potential, light,[19] temperature and ionic changes.[20] Bao *et al.* studied a 4-arm poly(ethylene glycol)-block-poly(L-glutamic acid) (4a-PEG-PLG) hydrogels and demonstrated that these hydrogels exhibits gel-sol transition due to pH change as shown in the Fig. **2**.

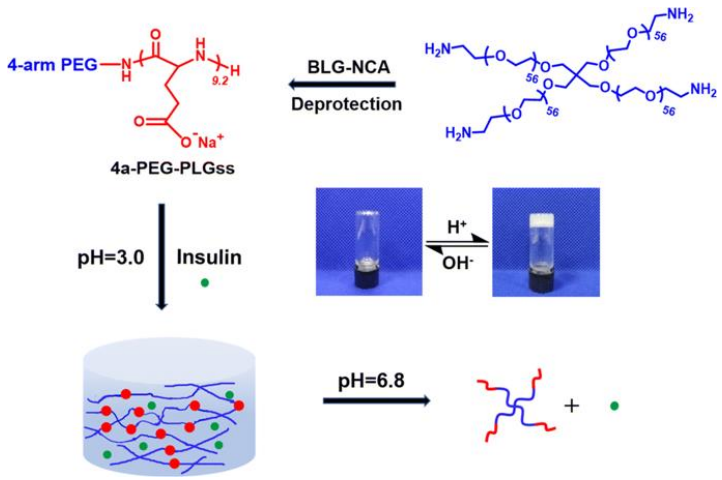

Fig. **2.** Insulin uptake and triggered release through a pH sensitive hydrogel.[21]

The response to these stimuli show changes in phase, physical structure, fluorescent properties, breakage of bonds or degradations[22,23] etc. and can be tuned by modifying the polymer chemistry. Compared to traditional drug delivery methods, these smart polymeric hydrogels can be used for drug delivery on demand. Stabenfeldt *et al.* reported the thermosensitive hydrogel based on methylcellulose which can be used for development of neural tissue scaffolds.[24] Likewise, numerous researchers are working on pH responsive, light-sensitive, or with multi-responsive hydrogels.[15] Fig. **3** given below shows an example of dual-responsive hydrogels which are sensitive to both light and reductive environment.

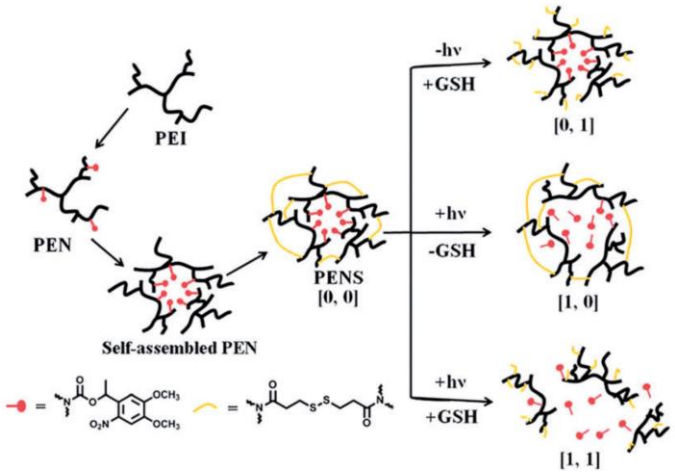

Fig. **3**. Dual-responsive nitrobenzyl-modified-polyetherimide crosslinked with dithiodipropionic acid (PENS) and their sensitivity to light and glutathione (GSH).[15]

Gluthione-sensitive hydrogels are researched mostly for cancer drug applications.[25-26] Cancer drug delivery has been a great challenge due to presence of various complex cell environments which negatively result the outcome of therapeutics drugs. For example, glutathione, a tripeptide that contains cysteine, is found at around relatively low concentration (~2-20μM) in plasma. However, in cancerous environments, it can be found at higher levels (~10mM).[27,28] Glutathione predominantly presents in cells in its reduced state (GSH). Despite GSH's beneficial role in the removal of carcinogens and protection from cell death, higher concentration can have pathogenic effect on cells leading to cancer progression.[29] GSH has been utilized to design thiol responsive therapeutic drugs delivery system.[30-31] Li and coworkers presented the release of drugs from micelles triggered by the high concentration GSH *via* the breakage of disulfide bond crosslinks. Baldwin *et al.* have reported the glutathione-sensitive hydrogels formed by various thiol-functionalized poly(ethylene glycol) crosslinked with maleimide functionalized low-molecular weight heparin. This study demonstrated that the

succinimide-thioether linkages added to the maleimide-functionalized heparin will be cleaved by various alkyl thiols along with glutathione (GSH) via thiol-exchange reaction.

Dithiomaleimide (DTM) is a fluorescent functional group formed on various substituted maleimides. O'Reilly *et al.* showed DTM-functional acrylate based nanoparticles via ROP and RAFT polymerization.[32-33]

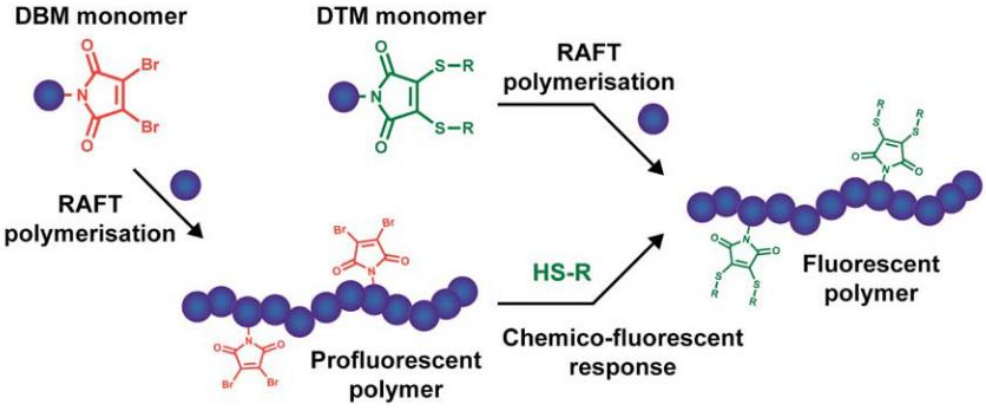

Fig. **4**. Schematic illustration of DTM monomer based fluorescent polymer and chemico-fluorescent response of dibromomaleimide (DBM) monomer based profluorescent polymer via RAFT polymerization.[33]

DTM derivative functionalized with thiols were shown to have a significant fluorescence shift.[34] Hence, Karman *et al.* utilized DTMs to devise a polymer that can show mechanically switchable fluorescence properties.[35] By incorporating DTM moiety into each chain of polymethylacrylate and of poly(ε-caprolactone), the cleavage of C-S bond of DTM was shown using ultrasonic-induced mechanical stress. In addition, DTM can be used for thiol exchange reaction. Smith *et al.* have shown that the DTM could undergo thiol-exchange reactions by replacement of original thiol linkage with the new thiol linkage.[36,33] The maleimide group of DTM facilitates the conjugation addition-elimination reaction due to the retention of the C=C double bond. Tang *et al.* developed a

poly(tri-ethylene glycol methyl ether acrylate) (PTEGA) based polymer with pendant DTM functionality using copper Cu(0)-mediated living radical polymerization. The pendent DTM were utilized for sequential reversible thiol-exchange reactions. Thiol exchange was successfully shown in presence of both alkylthiols such as GSH, as well as aryl thiols.

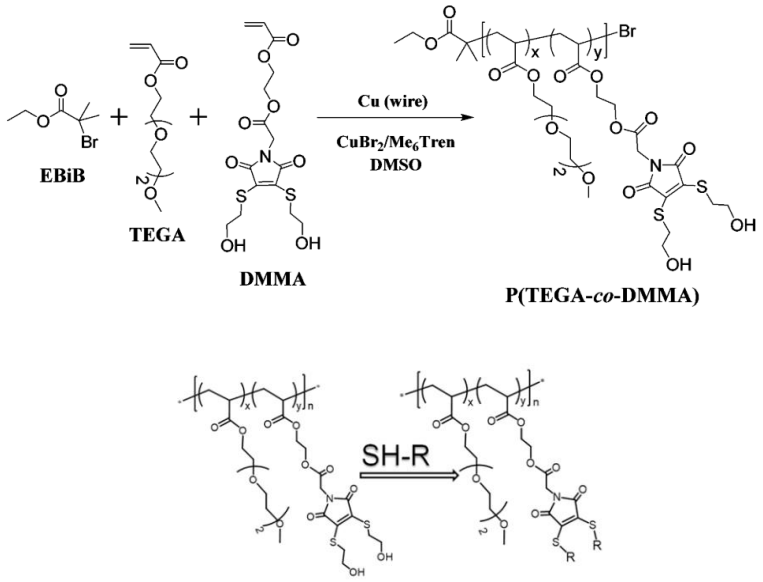

Fig. **5.** Schematic of copolymerization of P(TEGA-co-DMMA) polymer (Top) and thiol-exchange reaction of P(TEGA-co-DMMA) polymer with thiol containing agent (bottom).

This work attempts to utilize DTM as a crosslinker for the photopolymerization of thiol-sensitive poly(ethylene glycol) based hydrogel, namely, poly(ethylene glycol) methyl ether acrylate. We hypothesize the degradation of thiol linkages formed by functionalization of the DTM crosslinker, occurs via thiol exchange reaction with the alkyl thiol molecules including glutathione (GSH). The gelation and degradation kinetics are obtained by using combined study of oscillatory rheology and submersion dynamic

mechanical analysis. The reaction kinetics as well as dissolution kinetics is examined to understand the reaction rate and its respective mechanical behavior.

Chapter 2: Materials and methods

2.1 Materials

All reagents and solvents were bought from commercially available sources and used as received unless otherwise noted.

2.2 Instrumentation

^{1}H NMR was recorded on Varian Mercury 300 MHz spectrometer either with $CDCl_3$, D_2O, or acetone-D_6. Chemical shifts (δ) are reported in parts per million (ppm). The flash column chromatography was performed using Biotage Isolera Prime system. UV curing was performed using Bluepoint 4.0 with mercury UV lamp (150 W) at an intensity of 8 mW/cm^2. Rheology experiments were performed on TA ARES strain-controlled rheometer with an Omnic UV lamp attachment. A sample holder with 20 mm diameter was used for rheology experiments.

2.3 Methods

2.3.1 Synthesis of 1-benzyl-3,4-dibromo-1*H*-pyrrole-2,5-dione (1)

N-benzyl-functionalized dibromomaleimide was synthesized following the same procedure from the literature.[35] In short, 1 eq. of 2,3-dibromomaleimide (5 g, 19.6 mmol), 1.2 eq. of potassium carbonate (3.25 g, 28.5 mmol) and acetone (100 mL) was combined in a 250 mL round bottom flask under N_2. 1.25 eq. of benzyl bromide (3 mL, 25.3 mmol) was added dropwise and the solution was stirred overnight at the room temperature. The reaction mixture was concentrated *via* rotary evaporation to obtain a dry brown powder. The crude product was dissolved in EtOAc (150 mL), washed with water (3x50 mL) and

then brine (3x50 mL). Finally, the organic layer was then dried over $MgSO_4$, filtered and concentrated in *vacuo*. The product was purified using column chromatography (SiO_2, Hexane: EtOAc, elution gradient 7% EtOAc) solvent was removed with rotatory evaporation to obtain off-white powder product (3.8 g, 51.6 %).

^{1}H NMR ($CDCl_3$, ppm): δ= 4.75 (2H,s), 7.36 (5H, m); ^{13}C NMR ($CDCl_3$, ppm): δ= 43.22, 127.66, 128.31, 128.77, 129.48, 135.18, 158.65, 163.59.

2.3.2 Synthesis of 1-benzyl-3,4-bis(2-hydroxyethylthio)-1*H*-pyrrole-2,5-dione (2)

In a 25 mL round bottom flask, 1 eq. of **1** (3.8 g, 11 mmol) and 2.25 eq. imidazole (1.8 g, 27.5 mmol) were dissolved with THF (44 mL). With addition of 2.25 eq. mercaptoethanol (1.93 mL, 27.5 mmol) into the reaction mixture, solid precipitate formed immediately. After stirring for 3 hours, the precipitate was dissolved with EtOAc (200 mL) and washed with water (2x200 mL) and brine (3x200 mL). The organic layer was dried over $MgSO_4$ and filtered. The obtained filtrate was concentrated *via* rotary evaporation. The product was purified using column chromatography (SiO_2, hexanes, DCM, methanol, elution gradient from 25 % to 40% DCM and 2-5% MeOH). The solvent was removed with rotary evaporation and dried under vacuum at 40 °C overnight to obtain yellow colored **2** (1.8 mg, 55%).

^{1}H NMR ($CDCl_3$, ppm): δ= 3.59 (4H, t), 4.39 (4H, t), 4.65 (2H, s), 7.35 (5H, m); ^{13}C NMR ($CDCl_3$, ppm): δ= 34.55, 42.27, 61.97, 127.95, 128.35, 128.74, 135.88, 136.29, 166.34.

2.3.3 Synthesis of ((1-benzyl-2,5-dihydro-1*H*-pyrrole-3,4diyl)bis(sufanediyl))bis(ethane-2,1tea-diyl) diacrylate (3)

In a dry 250 mL round bottom flask, was combined **2** (1.8 g, 5.30 mmol), DCM (70 mL), and TEA (1.85 mL, 13.36 mmol). The solution was set in an ice bath and acryloyl chloride (1.07 mL, 13.26 mmol) was added dropwise under nitrogen. The solution was allowed to warm to room temperature and stir overnight. The reaction was washed with HCl (2x50 mL) followed by $NaHCO_3$ (2x50 mL), and brine (3x50 mL) before it was dried with $MgSO_4$ and filtered. The filtrate was purified using flash column chromatography (SiO_2, hexane: EtOAc, elution gradient from 0% to 25 % EtOAc) and solvent was removed using rotary evaporation to obtain yellow oil (1.3 g, 55%).
^{1}H NMR ($CDCl_3$, ppm): δ= 3.59 (4H, t), 4.39 (4H, t), 4.65 (2H, s), 5.81 (2H, d), 6.03 (2H, m), 6.34 (2H, d), 7.35 (5H, m).

2.4 Preparation of fully crosslinked networks

Poly(ethylene glycol) methyl ether acrylate (1.09 g, 2.27 mmol) with either ethylene glycol dimethacrylate (EGDMA) or **3** (0.001 g, 0.13 mmol) and 3 w% photoinitiator DMPA (0.03 g, 0.13 mmol) were combined in a scintillation vial. After quickly mixing, the solution is poured into a mold (Slygard 184) and photopolymerized using Bluepoint 4.0 with mercury UV lamp (150 W) at an intensity of 8 mW/cm^2 for 35 minutes.

2.5 ^{1}H NMR of hydrogels.

2.5.1 Formation

Gelation experiments were performed in a standard NMR tube with acetone-D_6 using Bluepoint 4.0 with mercury UV lamp (150 W) at an intensity of 8 mW/cm^2 at room temperature. NMR was taken before and after adding UV light to track the changes in the peak. In a standard NMR tube, PEG methyl ether acrylate ($1.6x10^{-2}$ g, $3.0x10^{-2}$ mmol), **3**

($1.6x10^{-5}$ g, $3.7x10^{-5}$ mmol), DMPA ($4.9x10^{-4}$ g, $1.9x10^{-3}$ mmol) were combined with an acetone-D_6 (0.5 mL). Measurements (32 scans, 5s delay, room temperature) for gelation were taken every 5 min of UV exposure until no acrylate peaks were seen. After 35 min of UV exposure, the reaction was stopped.

2.5.2 Degradation

Degradation experiments were performed on pre-made hydrogel sample in a standard NMR tube with deuterated water (D_2O). Glutathione (GSH) was used to monitor degradation via thiol-exchange reaction. In a standard NMR tube, a previously made C-**3** gel sample (12.5 mg) was immersed in a D_2O (0.5 mL) with 10 mM GSH. Degradation measurements (8 scans, room temperature) were taken every 5 min until acrylate peaks were seen. Time intervals were measured from thiol addition to beginning of NMR acquisition.

2.6 Sample holder for rheology experiment

Rheology experiments were performed using parallel plate geometry. To ensure accurate measurements, degradation tests were performed on hydrogels formed in the rheometer. Therefore, a modified parallel plate was utilized to allow for hydrogel submersion during degradation tests. The encapsulation of the bottom plate allows for submersion, while the high rim (above the bottom plate) prevents liquid runaway. Degradation solvents can be added into the sample chamber through the pinhole in the sidewall. The core circular diameter was 20 mm (0.79 inches) which has exact diameter of the rheometer parallel plate. The outside diameter was 28.6 mm (1.13 inches) whereas inside diameter was 26.34 mm (1.04 inches). The small circular pinhole for liquid

injection with 1.27 mm (0.05 inches) diameter was on the outside circular region such that the liquid injected falls on core region of the design. The material used for this design was aluminum.

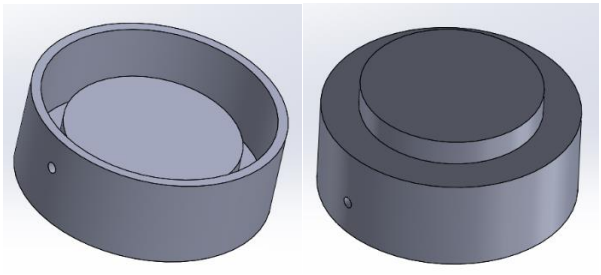

Fig. **6** sample holder 3D model

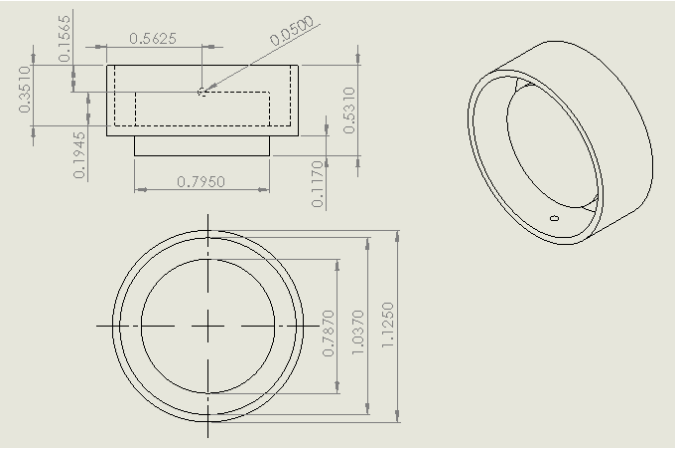

Fig. **7** Prototype drawing

2.7 Hydrogel formation monitored by oscillatory rheology

For each sample, polymer solution at 3 wt% photoinitiator, 0.1 w% crosslinker and were mixed and immediately loaded onto the sample holder through the small hole on the sample holder placed at the bottom instead of rheometer parallel plate. The oscillatory shear properties were measured using a TA ARES strain controlled rheometer with Omnic UV lamp at constant strain rate of 5.0%. Data was collected in a dynamic time sweep test at constant frequency of 1.0 rad s^{-1} at the room temperature until the

modulus reached equilibrium. The oscillatory rheology experiments is shown below in the Fig. **8**.

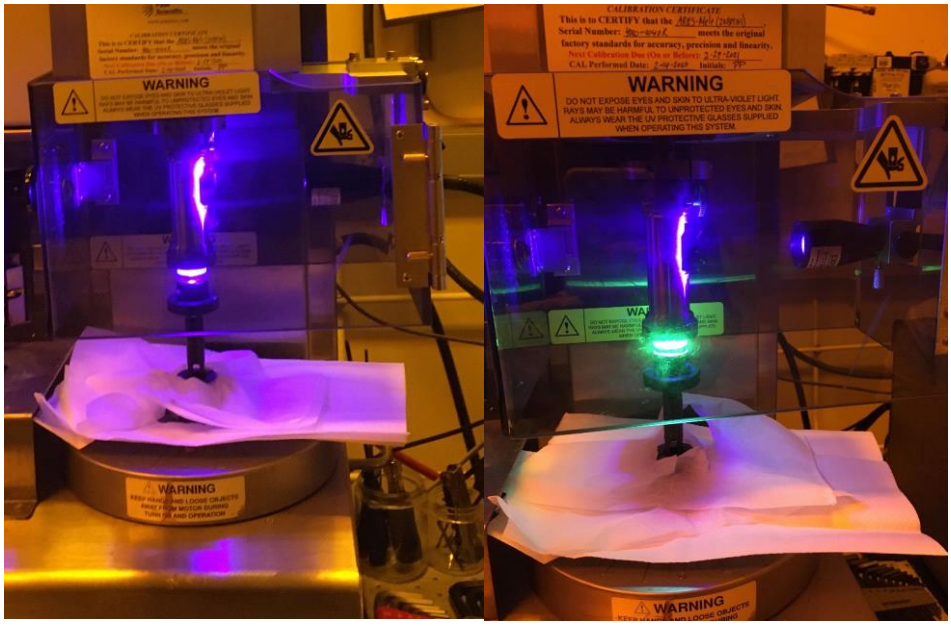

Fig. **8** Curing of C-EGDMA gel (left) and C-**3** gel (right) under UV light.

2.8 Hydrogel degradation monitored by oscillatory rheology

Degradation kinetics studies of the hydrogel in presence of thiol groups were measured based on the reduction in modulus with time. Hydrogels were formed in situ as described above. After the crosslinked hydrogel reached equilibrium, degradation measurements were performed by either immersion in pure PBS (pH 7.4), 10 mM GSH, or 10 mM mercaptoethanol by injection into the sample holder. Data points were recorded for 60 min.

Chapter 3: Result and discussion

3.1 Hydrogel formation by ^{1}H NMR

NMR studies have been used to study the gelation kinetics of hydrogels.[31] The hydrogel formation was monitored via ^{1}H NMR by tracking the acrylate proton peaks which disappear after fully crosslinking of the network.[31] Similar to the previously described procedure above, the formation of hydrogels with C-**3** crosslinkers was examined *via* ^{1}H NMR in acetone-D_6 solution with and without UV exposure. Formation studies were performed by exposing a standard NMR tube containing all the reactants to UV light in 5-minute increments up to total irradiance time of 35 minutes and schematic of hydrogel formation mechanism is shown in the Fig. **9**. The spectra in Fig. **10** shows the complete disappearance of the acrylate protons (6.34, 6.18 and 5.88 ppm) after 35 min of addition of photoinitiator which confirms that it is fully crosslinked. The peaks corresponding to photoinitator was seen around 7.5-8 ppm. Fig. **11** shows the normalized conversion of acrylate protons peaks at 5.88 ppm, 6.18 ppm and 6.34 ppm indicating the full conversion after 35 minutes of UV irradiation.

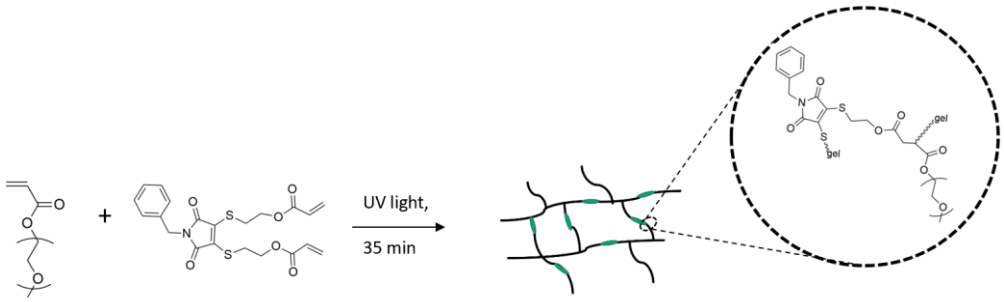

Fig. **9** C-**3** hydrogel formation mechanism.

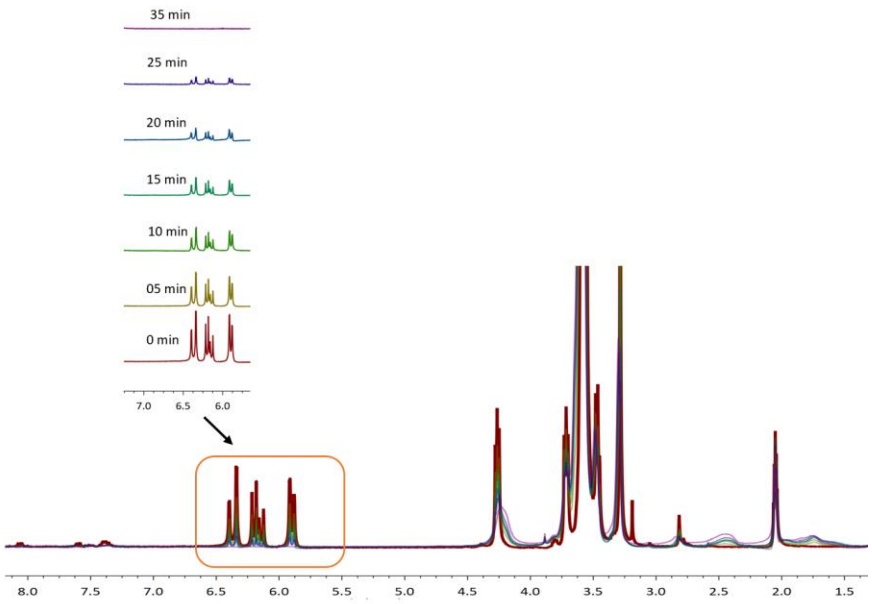

Fig. **10** ^{1}H NMR of C-**3** hydrogels formation. Experiments were performed in presence of acetone-D_6.

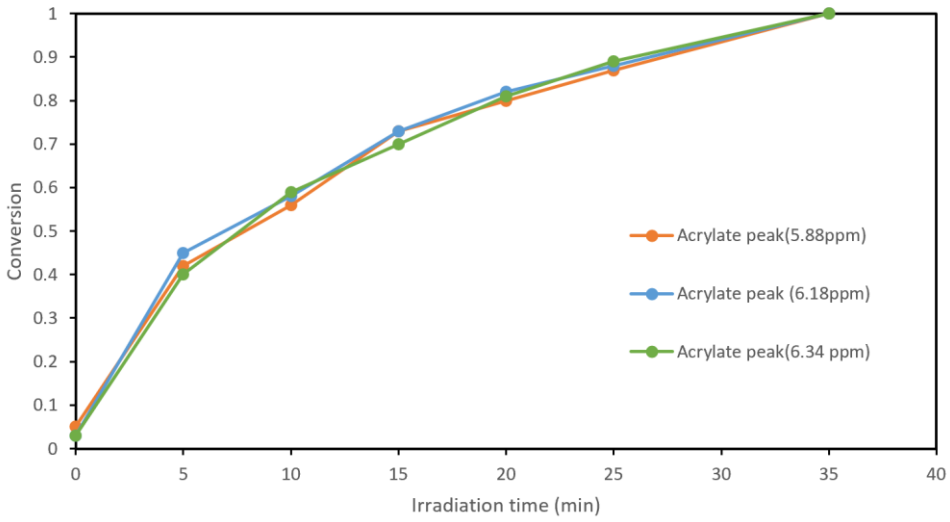

Fig. **11** Acrylate proton peaks conversion with UV irradiation for C-**3** gel within 35 min.

3.2 Degradation monitored by ^{1}H NMR

The hydrogel degradation kinetics were performed following literature procedure.[31] A fully formed C-**3** hydrogel (12.5 mg) was placed at the bottom of an NMR tube and submerged in D_2O with and without GSH (10 mM). The absence of acrylate proton peaks at 5.88-6.34 ppm shows that the gels was fully formed at the start of the experiments (0 min). The degradation kinetics were measured every 5 min after submersion for an hour and at 24 hr. The kinetics data before 10 mM GSH addition (0 min) and after thiol addition (20 min, 30 min, 40 min, 50 min, 60 min and 24 hr) are in Fig. **12**.

As the fully formed C-**3** hydrogel is subjected to thiol solution (10 mM GSH), a thiol peak should appear at around 1.50-1.70 ppm owing to the reversible thiol exchange indicating the degradation of the crosslinked networks. However, no peaks in this thiol region indicate that the degradation of the gel was not accomplished. Further study can be done by increasing the GSH concentration as well as increasing the reaction time which might help see the degradation of hydrogel.

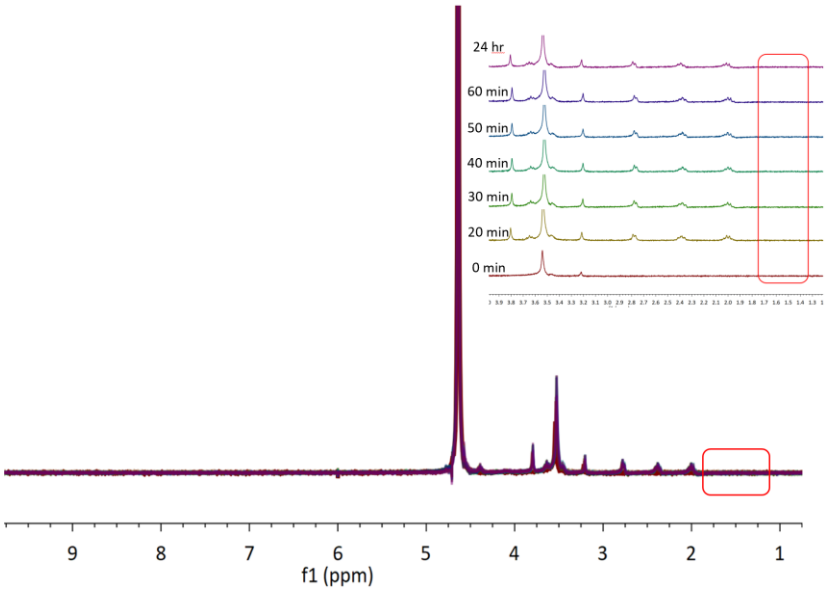

Fig. **12** ^{1}H NMR of PEG acrylate hydrogel degradation. Degradation kinetics experiments were performed in 10 mM GSH.

3.3 Rheological analysis of hydrogel formation

Oscillatory rheology was used to determine the gelation kinetics, mechanical properties and crosslink density of hydrogel. Hydrogels were either made with EGDMA crosslinker (C-EGDMA) or with the DTM crosslinker **3** (C-**3**). Full curing was defined as when the storage modulus (G'_{eq}) plateaus. Gelation was determined from crossing point of storage modulus (G') over loss modulus (G'') as shown in the Fig. **13**. The measured equilibrium storage moduli (G'_{eq}) for C-EGDMA hydrogel and C-**3** hydrogel were 8112 Pa and 2517 Pa respectively. The C-EGDMA hydrogel hits gelation within 65 s whereas C-**3** hydrogel took 80 s.

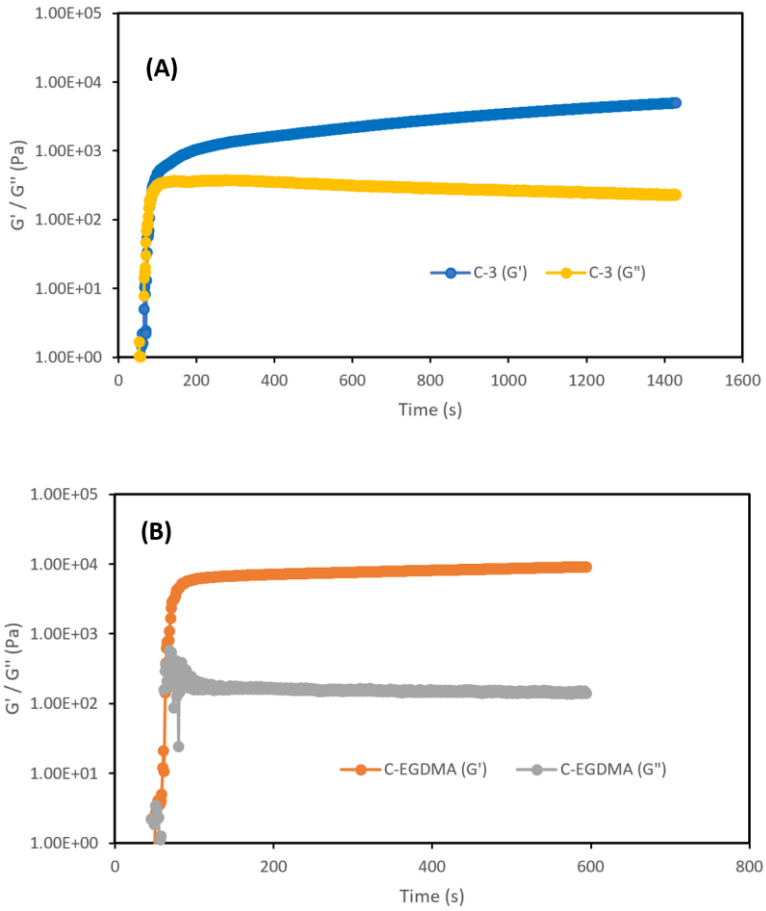

Fig. **13** Comparison of storage modulus (G′) versus loss modulus (G″) of C-**3** hydrogel (**A**) and C-EGDMA hydrogel (**B**) during curing process under UV. For each sample, the pre-mixed reaction was injected into the sample holder in rheometer with 20 mm thickness between two plates.

Fig. **14** shows the shorter gelation time for C-EGDMA hydrogels whereas longer gelation time for C-**3** hydrogel. This suggests that the C-EGDMA hydrogel has faster polymerization rate. The storage modulus (G′) is increasing slowly and exceeds the loss modulus (G″) curve reaching the gelation because of the establishment of the more networks, where solid-like viscoelastic behavior predominates. As progress of time, both

G′ and G″ curves level off indicating the fully developed networks in the hydrogel. Both C-**3** hydrogel and C-EGDMA hydrogel has lower G″ than G′ (G′ > G″), characteristic of a fully-developed crosslinked polymer network.[37] The lower storage modulus (G′) of C-**3** hydrogel as compared to C-EGDMA hydrogel shows that it is softer, and more elastic. Fig. **14** (**B**) shows the sharp increase in loss modulus within 50 s as a result of random error. There was a slight fluctuation in the instrument while running the experiments that eventually level off after adjustment.

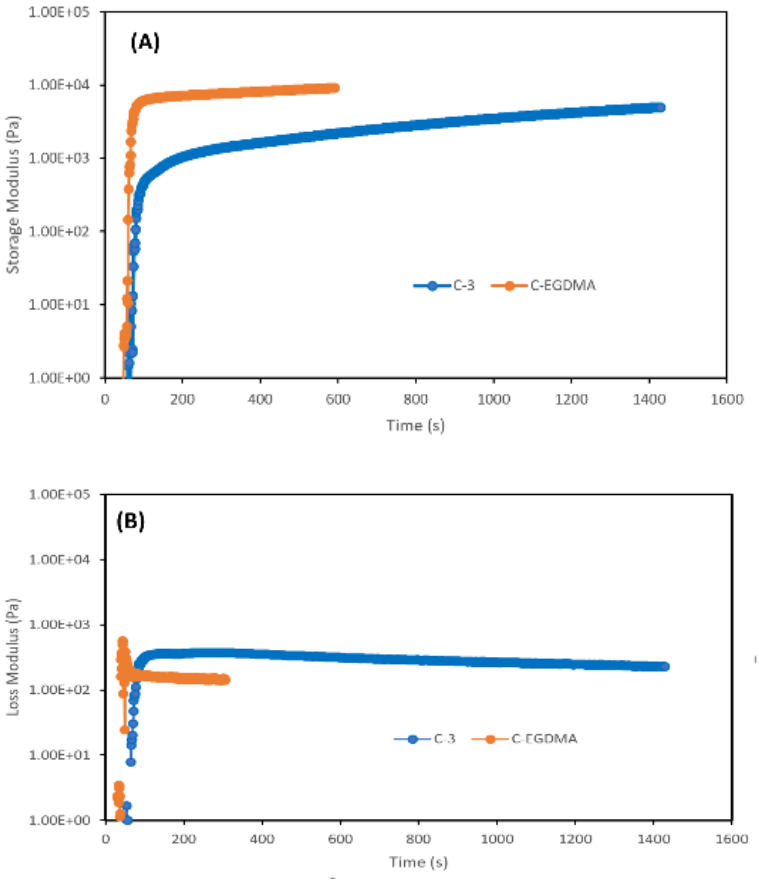

Fig. **14** Comparison of storage modulus (**A**) and loss modulus (**B**) of C-EGDMA versus C-**3** hydrogels during curing process under UV. For each sample, the pre-mixed

reaction was injected into the sample holder in rheometer with 20 mm thickness between two plates.

3.4 Rheological analysis of hydrogel degradation

Oscillatory rheology can be used to assess the kinetics and change in viscoelastic properties during the process of degradation.[38] The degradation of hydrogel was confirmed with reduction of the elastic modulus (G′). With the breakages of bonds of crosslinked networks via thiol exchange reaction, the elastic or storage modulus should decrease. To monitor the viscoelastic behavior of the hydrogel in presence of mercaptoethanol and GSH, two samples i.e. hydrogel with EGDMA crosslinker (C-EGDMA) and crosslinker **3** (C-**3**) were tested.

Fig. **15** shows the slight reduction of a normalized storage modulus versus time for both C-EGDMA and C-**3** hydrogel in presence of pure PBS, 10 mM GSH as well as 10 mM mercaptoethanol. The reduction in storage modulus (G′) of C-**3** hydrogel was similar to that of C-EGDMA hydrogel which indicates the initial radial swelling, since the C-EGDMA has no thiol exchange mechanism. Furthermore, the C-**3** hydrogel is expected to have sharp drop in G′ in presence of thiol solution because of thiol exchange whereas no change of G′ in pure PBS. However, there was no difference on storage modulus drop in presence of thiol solution (GSH or mercaptoethanol) versus pure PBS. This confirms further that the G′ drop seen for the C-**3** hydrogel is not because of hydrogel degradation but swelling. Due to instrument limitation, the experiment was only performed for an hour. Increasing the crosslinker wt% will increase the crosslink density which may lead to a larger drop in storage modulus with the course of degradation and

could be easier identify. However, the higher storage modulus expected for crosslink densities may require submersion clamp DMA.

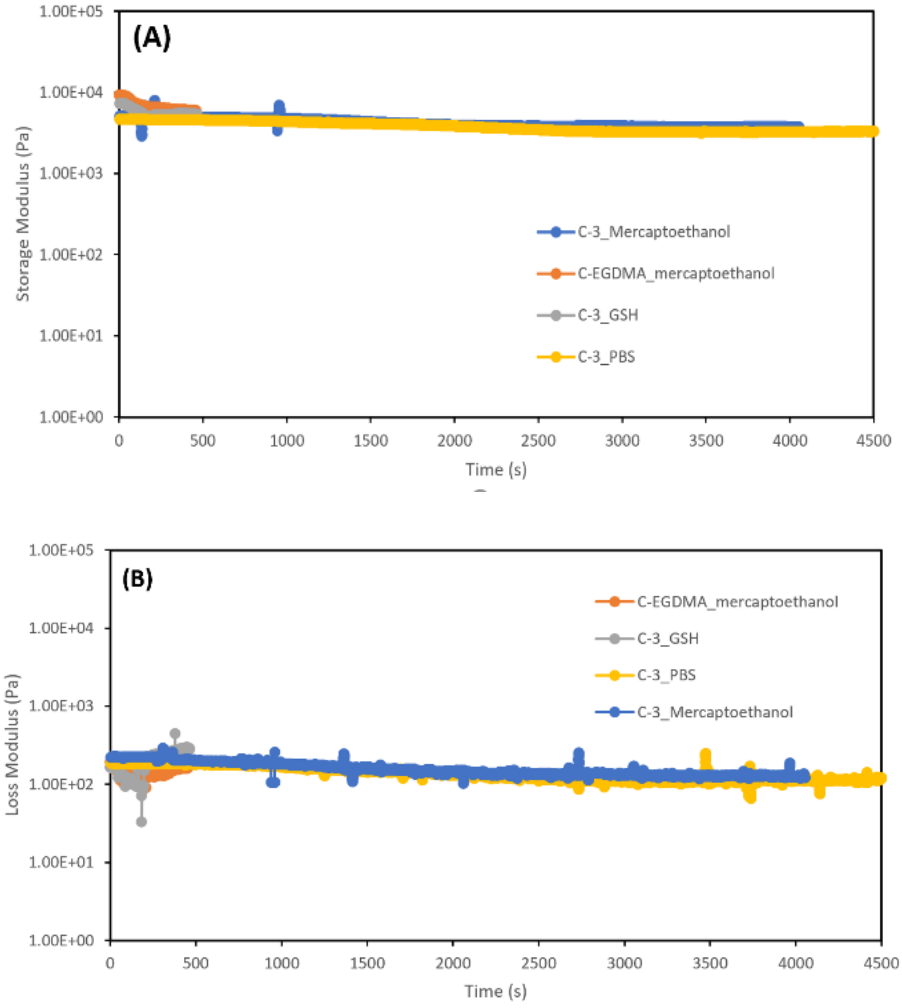

Fig. **15** Comparison of (**A**) storage and (**B**) loss modulus of C-EGDMA hydrogel and C-**3** hydrogel for degrading hydrogels. Degradation was performed in the presence of phosphate buffer saline (PBS, pH 7.4) solution (10 mM GSH, 10mM mercaptoethanol, pure PBS).

3.5 Determination of crosslink density of hydrogels

Crosslink density of hydrogel can be determined from two ways i.e. swelling experiments and rheological experiments.[39] As compared to swelling experiments, rheological experiments are known to provide optimal polymerization conditions due to in situ gelation.[37] The crosslink densities of the hydrogels were calculated using eq.1 and eq.3 obtained from the rheology experiments. By applying the theory of rubber elasticity, the average molecular weight between crosslinks (Mc) is defined as;[40]

$$Mc = \frac{\rho RT}{G'eq} \quad (1)$$

where ρ is the density of the gel and G'eq is the plateau modulus. The density of the gel (ρ) was calculated using Mettler Toldeo balance *via* Archemedes' principle. C-**3** gel has density of 1.20 g/mL whereas, density of C-EGDMA gel was 1.15 g/mL. The constant parameter used in this equation are the universal gas constant (R) and temperature (T) in Kelvin (K). R and T used were 8314 L Pa K^{-1} mol^{-1} and 298 K respectively. Jiang *et al.* demonstrated that the crosslink density of the highly swollen polyacrylate hydrogels can be calculated using alternative equation;[41]

$$G'eq = \rho_{\text{crosslinks}}\,\text{RT} \quad (2)$$

Combining the eq.1 and eq.2, the crosslink density equation was formulated as given below;

$$(\rho_{\text{crosslinks}}) = \frac{1}{\nu Mc} \quad (3)$$

where ν is specific density and calculated as the ratio of density of water to density of a gel. The crosslink density of C-**3** hydrogel (1.01×10^{-6} mol mL^{-1}) was lower than that of C-EGDMA hydrogel (3.27×10^{-6} mol mL^{-1}) which indicates that C-**3** hydrogel is softer as compared to C-EGDMA hydrogel which is in agreement with the rheological results.

Chapter 4: Conclusion

Hydrogels containing maleimide-thioether crosslinks were successfully fabricated from poly(ethylene glycol) methyl ether acrylate, acrylate functionalized DTM via photopolymerization. ^{1}H NMR analysis of hydrogel formation confirmed the complete disappearance of the acrylate double bond during crosslinking and validated the fully crosslinked networks. Oscillatory rheology was used to track both the photocuring as well as degradation of the hydrogel. The degration of hydrogel occurs by thiol exchange reaction with the DTM crosslinker *via* submersion in either mercaptoethanol or glutathione. However, the degradation experiments (NMR and rheological) indicate that the hydrogel degradation in presence of alkyl thiols and glutathione did not occur within the timescale of the experiments. Results indicated that increasing the crosslinker concentration to reduce swelling as well as to improve degradable mechanical properties in the presence of thiols may be necessary.

References

(1) Ahmed, E. M. Hydrogel: Preparation, Characterization, and Applications: A Review. *J. Adv. Res.* **2015**, *6* (2), 105–121.

(2) Graham, N. B.; McNeill, M. E. Hydrogels for Controlled Drug Delivery. *Biomaterials* **1984**, *5* (1), 27–36.

(3) Drury, J. L.; Mooney, D. J. Hydrogels for Tissue Engineering: Scaffold Design Variables and Applications. *Biomaterials* **2003**, *24* (24), 4337–4351.

(4) Akhtar, M. F.; Hanif, M.; Ranjha, N. M. Methods of Synthesis of Hydrogels: A Review. *Saudi Pharm. J.* **2016**, *24* (5), 554–559.

(5) Balakrishnan, B.; Banerjee, R. Biopolymer-Based Hydrogels for Cartilage Tissue Engineering. *Chem. Rev.* **2011**, *111* (8), 4453–4474.

(6) Jaipan, P.; Nguyen, A.; Narayan, R. J. Gelatin-Based Hydrogels for Biomedical Applications. *MRS Commun.* **2017**, *7* (3), 416–426.

(7) Coviello, T.; Matricardi, P.; Marianecci, C.; Alhaique, F. Polysaccharide Hydrogels for Modified Release Formulations. *J. Control. Release* **2007**, *119* (1), 5–24.

(8) Sharifi, F.; Patel, B. B.; McNamara, M. C.; Meis, P. J.; Roghair, M. N.; Lu, M.; Montazami, R.; Sakaguchi, D. S.; Hashemi, N. N. Photo-Cross-Linked Poly(Ethylene Glycol) Diacrylate Hydrogels: Spherical Microparticles to Bow Tie-Shaped Microfibers. *ACS Appl. Mater. Interfaces* **2019**, *11* (20), 18797–18807.

(9) Egami, M.; Haraguchi, Y.; Shimizu, T.; Yamato, M.; Okano, T. Latest Status of the Clinical and Industrial Applications of Cell Sheet Engineering and Regenerative

Medicine. *Arch. Pharm. Res.* **2014**, *37* (1), 96–106.

(10) Michida, N.; Hayashi, M.; Hori, T. Comparison of Event Related Potentials with and without Hypnagogic Imagery. *Psychiatry Clin. Neurosci.* **1998**, *52* (2), 145–147.

(11) Nguyen, K. T.; West, J. L. Photopolymerizable Hydrogels for Tissue Engineering Applications. *Biomaterials* **2002**, *23* (22), 4307–4314.

(12) Mohite, P. B.; Adhav, S. S. A Hydrogels : Methods of Preparation and Applications. *Int. J. Adv. Pharm.* **2017**, *06* (03), 79–85.

(13) Revzin, A.; Russell, R. J.; Yadavalli, V. K.; Koh, W. G.; Deister, C.; Hile, D. D.; Mellott, M. B.; Pishko, M. V. Fabrication of Poly(Ethylene Glycol) Hydrogel Microstructures Using Photolithography. *Langmuir* **2001**, *17* (18), 5440–5447.

(14) Kahn, J. S.; Hu, Y.; Willner, I. Stimuli-Responsive DNA-Based Hydrogels: From Basic Principles to Applications. *Acc. Chem. Res.* **2017**, *50* (4), 680–690.

(15) Knipe, J. M.; Peppas, N. A. Multi-Responsive Hydrogels for Drug Delivery and Tissue Engineering Applications. *Regen. Biomater.* **2014**, *1* (1), 57–65.

(16) Liang, Y.; Zhao, X.; Ma, P. X.; Guo, B.; Du, Y.; Han, X. PH-Responsive Injectable Hydrogels with Mucosal Adhesiveness Based on Chitosan-Grafted-Dihydrocaffeic Acid and Oxidized Pullulan for Localized Drug Delivery. *J. Colloid Interface Sci.* **2019**, *536*, 224–234.

(17) Li, M.; Tang, Z.; Sun, H.; Ding, J.; Song, W.; Chen, X. PH and Reduction Dual-Responsive Nanogel Cross-Linked by Quaternization Reaction for Enhanced Cellular Internalization and Intracellular Drug Delivery. *Polym. Chem.* **2013**, *4* (4), 1199–1207.

(18) Liu, Z.; Xu, G.; Wang, C.; Li, C.; Yao, P. Shear-Responsive Injectable Supramolecular Hydrogel Releasing Doxorubicin Loaded Micelles with PH-Sensitivity for Local Tumor Chemotherapy. *Int. J. Pharm.* **2017**, *530* (1–2), 53–62.

(19) Chen, X.; Liu, Z.; Parker, S. G.; Zhang, X.; Gooding, J. J.; Ru, Y.; Liu, Y.; Zhou, Y. Light-Induced Hydrogel Based on Tumor-Targeting Mesoporous Silica Nanoparticles as a Theranostic Platform for Sustained Cancer Treatment. *ACS Appl. Mater. Interfaces* **2016**, *8* (25), 15857–15863.

(20) Cao, Z.; Yang, Q.; Fan, C.; Liu, L.; Liao, L. Biocompatible, Ionic-Strength-Sensitive, Double-Network Hydrogel Based on Chitosan and an Oligo(Trimethylene Carbonate)-Poly(Ethylene Glycol)-Oligo(Trimethylene Carbonate) Triblock Copolymer. *J. Appl. Polym. Sci.* **2015**, *132* (35), 1–7.

(21) Bao, X.; Si, X.; Ding, X.; Duan, L.; Xiao, C. PH-Responsive Hydrogels Based on the Self-Assembly of Short Polypeptides for Controlled Release of Peptide and Protein Drugs. *J. Polym. Res.* **2019**, *26* (12).

(22) Gupta, P.; Vermani, K.; Garg, S. Hydrogels: From Controlled Release to PH-Responsive Drug Delivery. *Drug Discov. Today* **2002**, *7* (10), 569–579.

(23) Tang, Z.; Wilson, P.; Kempe, K.; Chen, H.; Haddleton, D. M. Reversible Regulation of Thermoresponsive Property of Dithiomaleimide-Containing Copolymers via Sequential Thiol Exchange Reactions. *ACS Macro Lett.* **2016**, *5* (6), 709–713.

(24) Li, M.; Mondrinos, M. J.; Chen, X.; Gandhi, M. R.; Ko, F. K.; Lelkes, P. I. Elastin Blends for Tissue Engineering Scaffolds. *J. Biomed. Mater. Res. Part A* **2006**, *79* (4), 963–973.

(25) Bai, T.; Du, J.; Chen, J.; Duan, X.; Zhuang, Q.; Chen, H.; Kong, J. Reduction-

responsive dithiomaleimide-based polymeric micelles for controlled anti-cancer drug delivery and bioimaging. *Polym. Chem.* **2017**, *8* (46), 7160–7168.

(26) Kapadia, C. H.; Tian, S.; Perry, J. L.; Luft, J. C.; Desimone, J. M. Reduction Sensitive PEG Hydrogels for Codelivery of Antigen and Adjuvant to Induce Potent CTLs. *Mol. Pharm.* **2016**, *13* (10), 3381–3394.

(27) Wu, G.; Fang, Y.-Z.; Yang, S.; Lupton, J. R.; Turner, N. D. Glutathione Metabolism and Its. *J. Nutr.* **2004**, *134* (3), 489–492.

(28) Jones, D. P.; Carlson, J. L.; Samiec, P. S.; Sternberg, P.; Mody, V. C.; Reed, R. L.; Brown, L. A. S. Glutathione Measurement in Human Plasma. Evaluation of Sample Collection, Storage and Derivatization Conditions for Analysis of Dansyl Derivatives by HPLC. *Clin. Chim. Acta* **1998**, *275* (2), 175–184.

(29) Bansal, A.; Celeste Simon, M. Glutathione Metabolism in Cancer Progression and Treatment Resistance. *J. Cell Biol.* **2018**, *217* (7), 2291–2298.

(30) Li, R.; Peng, F.; Cai, J.; Yang, D.; Zhang, P. Redox Dual-Stimuli Responsive Drug Delivery Systems for Improving Tumor-Targeting Ability and Reducing Adverse Side Effects. *Asian J. Pharm. Sci.* **2019**.

(31) Baldwin, A. D.; Kiick, K. L. Reversible Maleimide-Thiol Adducts Yield Glutathione-Sensitive Poly(Ethylene Glycol)-Heparin Hydrogels. *Polym. Chem.* **2013**, *4* (1), 133–143.

(32) Robin, M. P.; Osborne, S. A. M.; Pikramenou, Z.; Raymond, J. E.; O'Reilly, R. K. Fluorescent Block Copolymer Micelles That Can Self-Report on Their Assembly and Small Molecule Encapsulation. *Macromolecules* **2016**, *49* (2), 653–662.

(33) Robin, M. P.; O'Reilly, R. K. Fluorescent and Chemico-Fluorescent Responsive

Polymers from Dithiomaleimide and Dibromomaleimide Functional Monomers. *Chem. Sci.* **2014**, *5* (7), 2717–2723.

(34) Mabire, A. B.; Robin, M. P.; Quan, W. D.; Willcock, H.; Stavros, V. G.; O'Reilly, R. K. Aminomaleimide Fluorophores: A Simple Functional Group with Bright, Solvent Dependent Emission. *Chem. Commun. (Camb).* **2015**, *51* (47), 9733–9736.

(35) Karman, M.; Verde-Sesto, E.; Weder, C.; Simon, Y. C. Mechanochemical Fluorescence Switching in Polymers Containing Dithiomaleimide Moieties. *ACS Macro Lett.* **2018**, *7* (9), 1099–1104.

(36) Smith, M. E. B.; Schumacher, F. F.; Ryan, C. P.; Tedaldi, L. M.; Papaioannou, D.; Waksman, G.; Caddick, S.; Baker, J. R. Protein Modification, Bioconjugation, and Disulfide Bridging Using Bromomaleimides. *J. Am. Chem. Soc.* **2010**, *132* (6), 1960–1965.

(37) Calvet, D.; Wong, J. Y.; Giasson, S. Rheological Monitoring of Polyacrylamide Gelation: Importance of Cross-Link Density and Temperature. *Macromolecules* **2004**, *37* (20), 7762–7771.

(38) Sun Han Chang, R.; Lee, J. C. W.; Pedron, S.; Harley, B. A. C.; Rogers, S. A. Rheological Analysis of the Gelation Kinetics of an Enzyme Cross-Linked PEG Hydrogel. *Biomacromolecules* **2019**, *20* (6), 2198–2206.

(39) Omidian, H.; Hashemi, S. A.; Askari, F.; Nafisi, S. Swelling and Crosslink Density Measurements for Hydrogels. *Iran. J. Polym. Sci. Technol.* **1994**, *3* (2), 115–119.

(40) Tsuji, Y.; Li, X.; Shibayama, M. Evaluation of Mesh Size in Model Polymer Networks Consisting of Tetra-Arm and Linear Poly(Ethylene Glycol)S. *Gels* **2018**, *4* (2), 50.

(41) Jiang, H.; Su, W.; Mather, P. T.; Bunning, T. J. Rheology of Highly Swollen Chitosan/Polyacrylate Hydrogels. *Polymer (Guildf).* **1999**, *40* (16), 4593–4602.

Appendix

NMR Spectra

1-benzyl-3,4-dibromo-1H-pyrrole-2,5-dione (1)

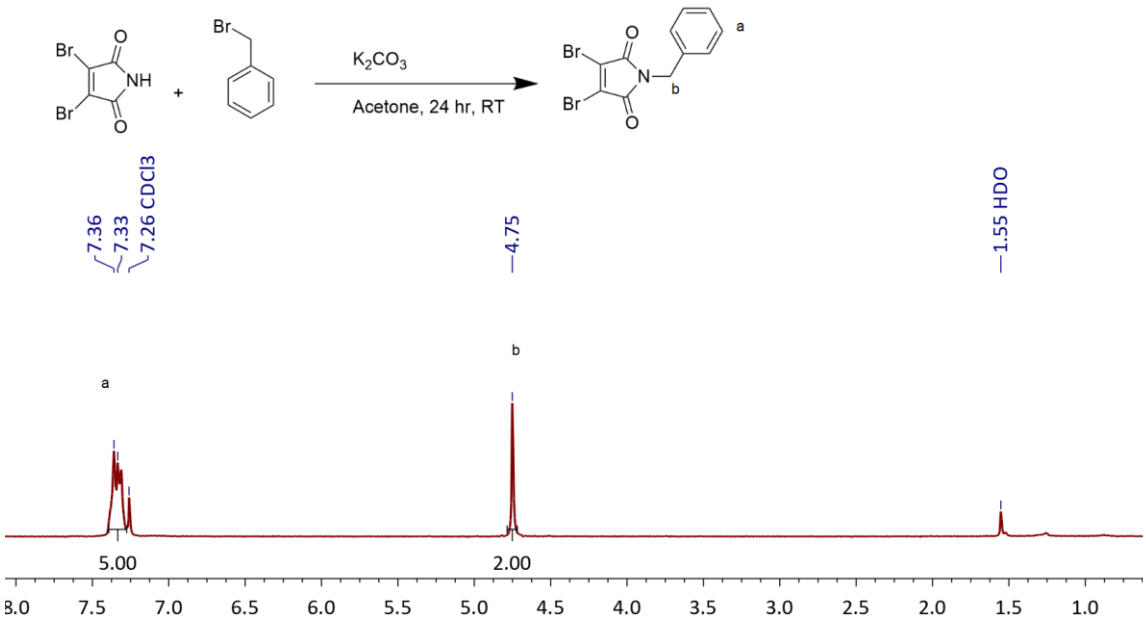

Fig. 9 ^{1}H NMR spectrum of **1** in $CDCl_3$.

1-benzyl-3,4-dibromo-1H-pyrrole-2,5-dione (1)

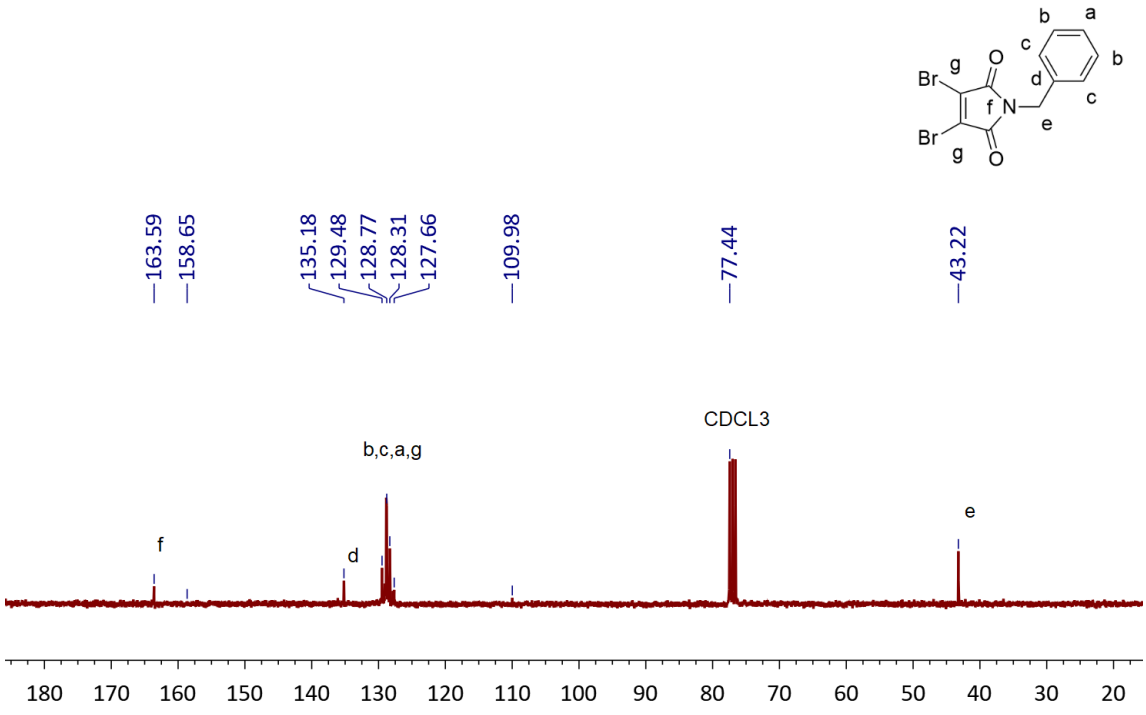

Fig. 10 ^{13C} NMR spectrum of **1** in $CDCl_3$.

1-benzyl-3,4-bis(2-hydroxyethylthio)-1H-pyrrole-2,5-dione (2)

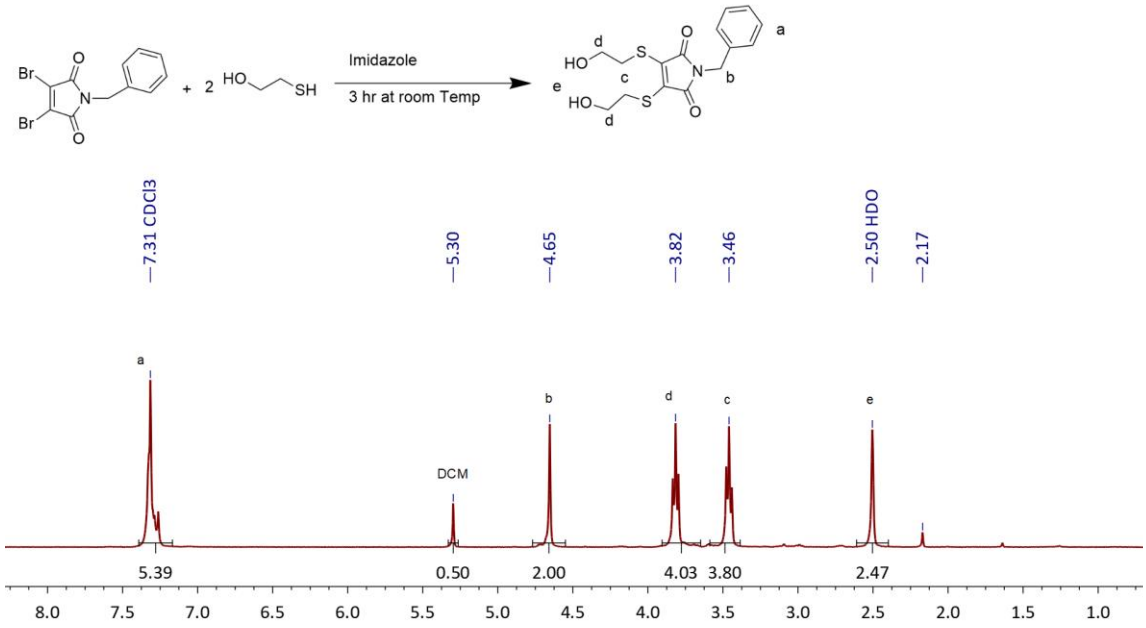

Fig. 11 ^{1}H NMR spectrum of **2** in $CDCl_3$.

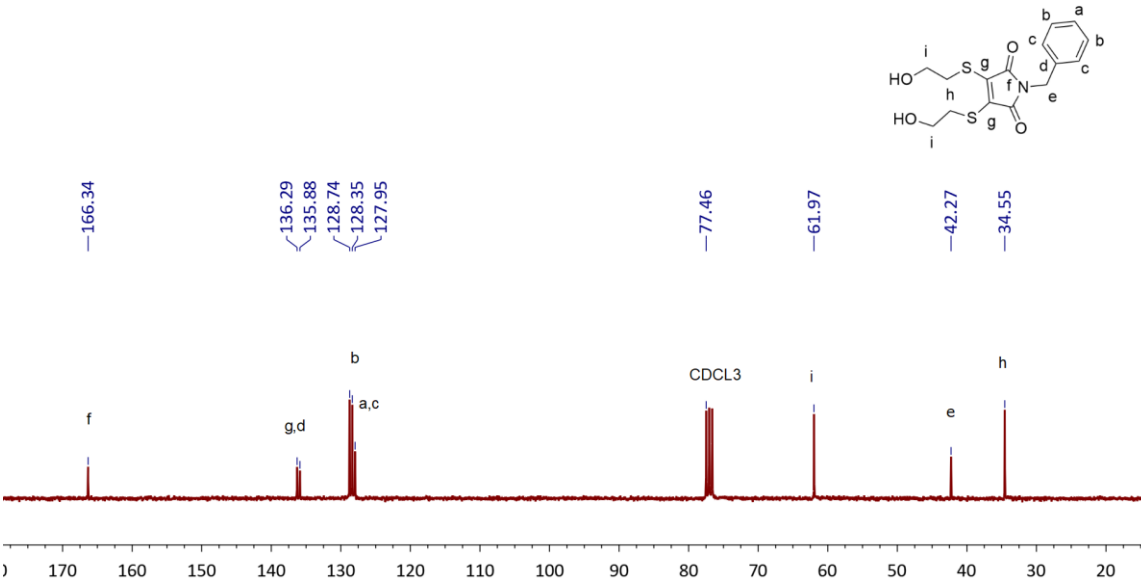

Fig. 12 ^{13}C NMR spectrum of **2** in $CDCl_3$.

2.3.3 Synthesis of ((1-benzyl-2,5-dihydro-1H-pyrrole-3,4diyl)bis(sulfanediyl))bis(ethane-2,1-diyl) diacrylate (3)

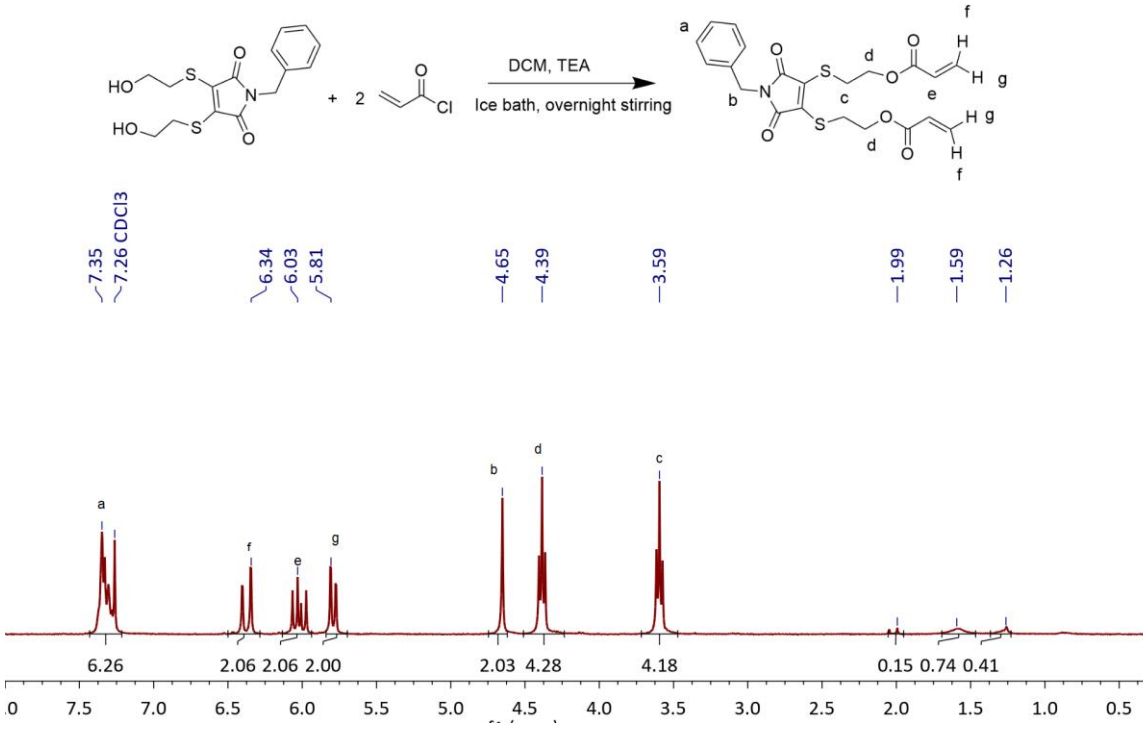

Fig. 12 ^{1}H NMR spectrum of **3** in $CDCl_3$.